Neutron Scattering: Theory, Instrumentation, and Simulation

Kim Lefmann
Department of Materials Research
Risø National Laboratory
Technical University of Denmark

August 25, 2007

Foreword and acknowledgements

These notes are written as lecture notes for a University course in Neutron Scattering, University of Copenhagen, autumn 2007. In contrast to most textbooks on this topic, these notes cover both theoretical and experimental aspects. Further, the notes contain material on ray-tracing simulations of neutron instruments.

The theoretical part of these notes are largely inspired by the classical textbooks by Marshall and Lovesey[1], and Squires[2], but the material has been simplified to make it appropriate for beginners in this field and re-organised in (for me) a more streamlined way. Further, this text contains more recent topics like small-angle scattering and simulations. It is intented to make the notation consistent with Squires[2], since this is used as a second sourcebook for the course. One major difference, though, is the use of q in stead of κ for the scattering vector, in order to make the notation compatible also for SANS.

I am strongly indepted to K.N. Clausen for introducing me to the secrets of neutron scattering and for support far beyond the duties and timespan of a Ph.D. supervisor. Without him this work would have been utterly impossible.

A wholehearted thank goes to R. McGreevy for providing me the "five reasons" for neutron scattering. R. McGreevy also led the EU project SCANS, which inspired and funded parts of the work related to computer simulations. He is also leading the EU NMI3 and ISIS-TS2 projects, presently supporting the simulation work.

I would at this point like to thank all persons who joined me in developing the McStas simulation package: Kristian Nielsen, Henrik M. Rønnow, Emmanuel Farhi, Per-Olof Åstrand, Peter K. Willendrup, Klaus Lieutenant, Peter Christiansen, and Erik Knudsen.

I thank J.O. Birk for drawing most of the illustrations. The remaining figures were provided by P.K. Willendrup, P. Christiansen, and R. McGreevy.

Contents

Chapter 1

Introduction to neutron scattering

Neutron scattering is one of the most powerful and versatile experimental methods to study the structure and dynamics of materials on the nanometer scale. Quoting the Nobel committe, when awarding the prize to C. Shull and B. Brockhouse in 1994: "Neutrons tell you where the atoms are and what the atoms do" [3].

Neutron scattering is presently used by more than 5000 researchers Worldwide, and the scope of the method is continuously broadening. 40 years ago, neutron scattering was an exotic tool for solid state physicists and crystallographers, but today it serves communities as wide as Biology, Earth Sciences, Planetary Science, Engineering, Nanoscience, and Cultural Heritage. In brief, neutrons are used in all scienfitic fields that deal with condensed matter.

It is, however, appropriate to issue a warning already here. Although neutron scattering is a great technique, it is also slow and expensive. Neutron scattering experiments last several days and are performed at large international facilities. Here, the running costs corresponds to thousands of Euros per instrument day. Hence, neutron scattering should be used only where other methods are inadequate.

For the study of atomic and nanometer-scale structure in materials, X-ray scattering is the technique of choice. X-ray sources are by far more abundant and are, especially for synchrotron X-ray sources, much stronger than neutron sources. Hence, the rule of thumb goes: "If an experiment can be performed with X-rays, use X-rays". For introduction to X-ray scattering, see, *e.g.*, the excellent recent textbook by D. F. McMorrow and J. Als-Nielsen [4].

The remainder of this chapter is devoted to presenting the properties of the neutron and describing the important differences between neutron and X-ray scattering.

1.1 Basic properties of the neutron

The neutron is a nuclear particle with a mass rather close to that of the proton

$$m_{\mathrm{n}} = 1.675 \cdot 10^{-27}\,\mathrm{kg}. \tag{1.1}$$

The neutron does not exist naturally in free form, but decays into a proton, an electron, and an anti-neutrino. The neutron lifetime, $\tau = 886$ s [5], is much longer than the time of a neutron within a scattering experiment, where each neutron spends merely a fraction of a second. The neutron is electically neutral but still possess a magnetic moment

$$\mu = \gamma \mu_{\mathrm{N}}, \tag{1.2}$$

where $\gamma = -1.913$ is the neutron magnetogyric ratio and the nuclear magneton is given by $\mu_{\mathrm{N}} = e\hbar/m_{\mathrm{p}}$. The neutron magnetic moment is coupled antiparallel to its spin, which has the value $s = 1/2$.

The neutron interacts with nuclei via the strong nuclear force and with magnetic moments via the electromagnetic force. Most of this text deals with the consequences of these interactions; *i.e.* the scattering and absorption of neutrons inside materials and reflection from their surfaces.

1.2 Particle-wave duality

One of the remarkable consequences of quantum mechanics is that matter can have both particle- and wave-like nature. The neutron is no exception from this. In neutron scattering experiments, neutrons behave as particles when they are created, as waves when they scatter, and again as particles when they are detected.

To be more specific, a particle moving with constant velocity, v, can be ascribed a corresponding (de-Broglie) wavelength, given by

$$\lambda = \frac{2\pi\hbar}{mv}, \tag{1.3}$$

where the Planck constant is $\hbar = 1.034 \cdot 10^{-34}$ Js. In neutron scattering, the wave nature is often referred to in terms of the neutron *wave number*, $k = 2\pi/\lambda$, or the *wave vector* of length k and with same direction as the velocity:

$$\mathbf{k} = \frac{m_{\mathrm{n}}\mathbf{v}}{\hbar}. \tag{1.4}$$

By tradition, wavelengths are measured in Å, wavenumbers in $\mathrm{Å}^{-1}$, while the neutron velocity is measured in SI units: m/s. For our purpose we consider the neutrons as non-relativistic, and the neutron kinetic energy is given by

$$E = \frac{\hbar^2 k^2}{2m_{\mathrm{n}}}, \tag{1.5}$$

which is measured in eV or meV, where 1 eV$= 1.602 \cdot 10^{-19}$ J. A useful conversion table between velocity, wave number, wavelength, and energy, is given as Table 1.2.[2]

	v [ms^{-1}]	λ^{-1} [Å^{-1}]	k [Å^{-1}]	$\sqrt{E}$ [meV$^{1/2}$]
v [ms^{-1}]	1	2.528×10^{-4}	1.588×10^{-3}	2.286×10^{-3}
λ^{-1} [Å^{-1}]	3956	1	6.283	9.045
k [Å^{-1}]	629.6	0.1592	1	1.440
$\sqrt{E}$ [meV$^{1/2}$]	437.4	0.1106	0.6947	1

Table 1.1: Conversion table between different neutron parameters in the most commonly used units. Example of use: $v\,[\mathrm{ms}^{-1}] = 629.6\,k\,[\mathrm{Å}^{-1}]$.

1.3 Neutron scattering facilities

Neutrons can be produced in a number of ways, e.g. as by-products of cosmic radiation or radioactive decay of heavy nuclei. More recently, neutrons have been produced in a laboratory experiment, using a piezoelectric crystal to accelerate ions of deuterium (the heavy hydrogen isotope ^{2}D) to high energies [8].

Neutron sources with flux densities adequate for neutron scattering investigations of materials are based on one of two principles, also illustrated in Fig. 1.1:

- **Fission.** A high continuous flux of neutrons is produced in the core of a conventional fission reactor. For neutron scattering purposes, research reactors with compact cores are used rather than the more abundant nuclear power plants.

- **Spallation.** By bombarding a target of heavy elements with high-energy particles (typically protons), a very large number of neutrons can be produced. Spallation sources are typically pulsed, but can also be pseudo-continuous, depending on the proton accelerator.

Common to both types of sources is that neutrons are being moderated to thermal velocities close to the source and then transported to the neutron scattering instruments in neutron guide systems.

Both types of neutron sources are built as dedicated facilities, each hosting tens of instruments. All major sources are user facilities, meaning that they serve a research community much larger than the staff employed at the facilities. Typically, user experiments are selected through a competitive proposal system.

At the time of writing, more than twenty neutron facilities are in operation Worldwide, the most important being the reactor source ILL, Grenoble, France, and the spallation source ISIS, Oxfordshire, UK. However, the European dominance is about to be challenged by the very powerful spallation sources under commisioning: SNS, Tennessee, USA, and J-PARC, Japan [6].

A list of the most significant neutron sources is given in Chapter 3.

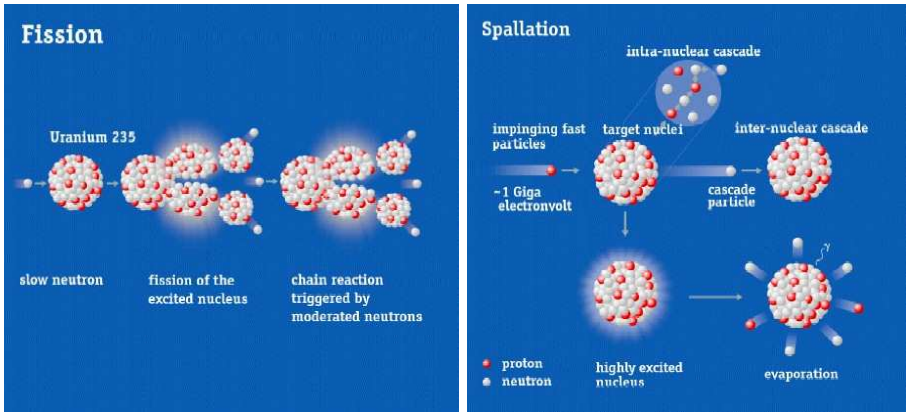

Figure 1.1: The two different ways of neutron production. Left: Traditional nuclear reactors make use of production of neutrons for maintaining the chain reaction; extra neutrons can be used for neutron scattering. Right: Protons accelerated into the GeV regime can split heavy nuclei with a large neutron surplus, creating free neutrons as a part of the reaction products.

1.4 Neutron scattering instruments and detectors

Neutron scattering instruments are build in many different designs, reflecting that they are specialized for vastly different research purposes. Some instruments deal with the study of the structure of crystals, other with excitations in materials, others again with the properties of thin films, and so forth.

In these notes, we will present the basic features in most of the commonly used instrument designs. We will, however, not go much into details with the way neutrons are detected. This is typically done by a nuclear reaction, which destoys the neutron as a result. The charged by-products gives rise to an electrical signal, which can be amplified and detected. The field of neutron detectors is vast and we refer the reader to more specialized literature for details [9].

1.5 Five reasons for using neutrons

At last in this introductory chapter, we will present some of the assetts of neutron scattering. We will focus on cases where neutrons can be prefered over X-rays. It is commonly agreed in the neutron scattering community that this can be formulated in five general points:

1. Thermal neutrons have a wavelength (2 Å) similar to inter-atomic distances, and an energy (20 meV) similar to elementary excitations in solids. One can thus obtain simultaneous information on the structure and dynamics of materials and *e.g.* measure dispersion relations (energy-wavelength

dependence) of excitations.

2. The neutron scattering cross section varies randomly between elements and even between different isotopes of the same element. One can thus use neutrons to study light isotopes. In particular, this is important for hydrogen, which is almost invisible with X-rays. With neutrons, the large difference in scattering between usual hydrogen (^{1}H) and deuterium, ("heavy hydrogen", ^{2}D) can be used in polymer- and biological sciences to change the contrast in the scattering and also "highlight" selected groups of large molecules.

3. The interaction between neutrons and solids is rather weak, implying that neutrons in most cases probe the bulk of the sample, and not only its surface. In addition, quantitative comparisons between neutron scattering data and theoretical models are possible, since higher-order effects are small and can usually be corrected for or neglected.

4. Since neutrons penetrate matter easily, neutron scattering can be performed with samples stored in all sorts of sample environment: Cryostats, magnets, furnaces, pressure cells, *etc.* Furthermore, very bulky samples can be studied, up to 10 cm thickness, depending on its elemental composition.

5. The neutron magnetic moment makes neutrons scatter from magnetic structures or magnetic field gradients. Unpolarized neutrons are used to learn about the periodicity and magnitude of the magnetic order, while scattering of spin-polarized neutrons can reveal the direction of the atomic magnetic moments.

In most cases, neutron scattering is performed in combination with other experimental techniques; often with neutron scattering as one of the final techniques to be used before conclusions can be drawn.

1.6 On this text

After this brief introduction, we will continue the general part by introducing the formalism of the neutron scattering process (chapter 2), go more into details with neutron sources, moderators, and guide systems (chapter 3), and with Monte Carlo ray-tracing techniques for describing the workings of neutron scattering instruments (chapter 4).

In the second part, we will describe the actual applications of neutron scattering. For each case, we give the necessary theoretical background, a description of the experimental set-up, and a number of corresponding problems, including instrument simulations. Small angle neutron scattering (SANS) is presented in chapter 5, diffraction from crystals in chapter 6, inelastic scattering from lattice vibrations (phonons) in chapter 7, and magnetic scattering in chapters 8 and 9. In the third part, to be written, we will describe a number of

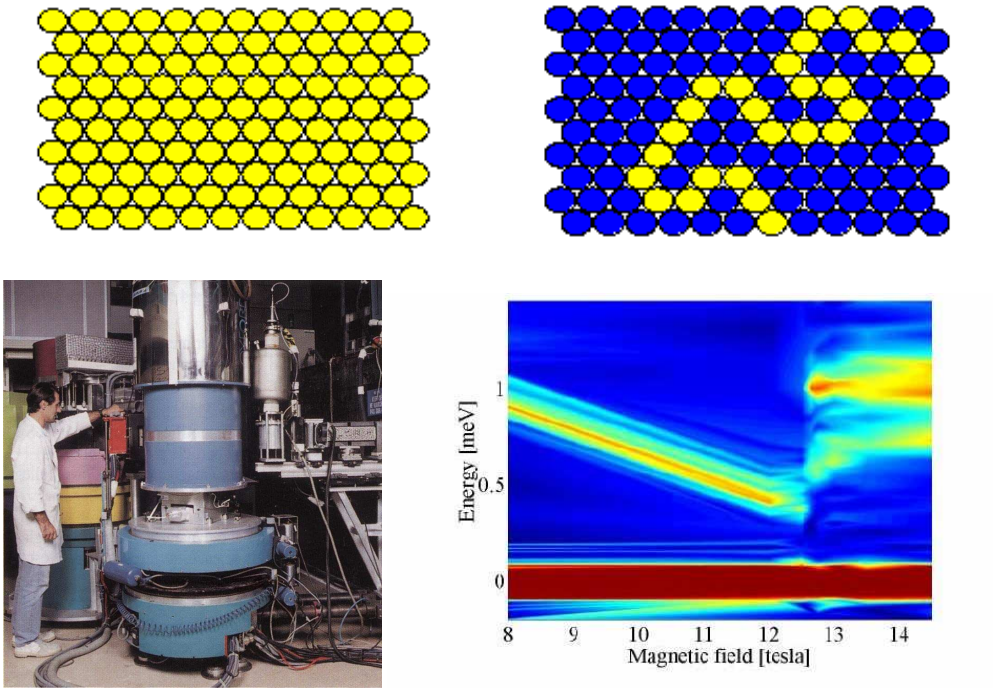

Figure 1.2: Illustration of some of the "five reasons" for neutron scattering. Top row shows schematically the neutron visibility of one polymer chain in two different solutions (left) hydrogenous solvent, (right) deuterated solvent. Bottom row shows the measurement of magnetic excitations as a function of applied magnetic field (right). To perform the measurements, the neutron beam must penetrate the Al walls of a large cryomagnet (left).

advanced utilizations of neutron scattering, like scattering with polarized neutrons and scattering from polarized nuclei.

Later extensions of the notes may include the topics radiography/tomography, reflectivity from surfaces, single crystal diffraction, quasielastic scattering from diffusion, scattering from liquids, and ultracold neutrons. It is also likely that chapters on neutron detectors, neutron optics, and analytical resolution calculations will be written.

Chapter 2

Basics of neutron scattering

This chapter contains the basics of neutron scattering formalism. Its contents forms the basis for the understanding of later chapters of neutron scattering from particular systems, like macromolecules, surfaces, crystals, etc.

The process of neutron scattering is unavoidably of quantum mechanical nature. However, the first part of this chapter is kept less rigorous, since for many applications a full formal treatment is unnecessary.

2.1 The neutron cross sections

We first introduce the terms by which we describe the scattering of a neutron beam. We define the flux of a neutron beam as

$$\Psi = \frac{\text{number of neutrons impinging on a surface per second}}{\text{surface area perpendicular to the neutron beam direction}}. \tag{2.1}$$

We then continue to describe the interaction of a neutron beam with materials by introducing the central concept of cross sections.

2.1.1 The scattering cross section

The *neutron scattering cross section*, σ, of a system is defined by its ability to scatter neutrons:

$$\sigma = \frac{1}{\Psi} \text{ number of neutrons scattered per second}, \tag{2.2}$$

which has units of area. The scattering cross section used here is the total cross section, which depends on the system (sample) size. For most samples, this can be described by the volume specific cross section, Σ, through

$$\sigma = V\Sigma. \tag{2.3}$$

2.1.2 The differential scattering cross section

The angular dependence of the scattered neutrons is a most important aspect of all neutron scattering. To describe this, we employ the *differential scattering cross section*:

$$\frac{d\sigma}{d\Omega} = \frac{1}{\Psi} \frac{\text{number of neutrons scattered per second into solid angle } d\Omega}{d\Omega}. \quad (2.4)$$

The total number of scattered neutrons is of course the sum of neutrons in all of the 4π solid angle, whence

$$\sigma = \int \frac{d\sigma}{d\Omega} d\Omega. \quad (2.5)$$

2.1.3 The partial differential scattering cross section

For describing inelastic scattering, one needs to take into account the energy dependence of the scattered neutrons. This is described by the *partial differential scattering cross section*:

$$\frac{d^2\sigma}{d\Omega dE_\mathrm{f}} = \frac{1}{\Psi} \frac{\text{no. of neutrons scattered per sec. in } d\Omega \text{ with energies } [E_\mathrm{f}; E_\mathrm{f} + dE_\mathrm{f}]}{d\Omega dE_\mathrm{f}}. \quad (2.6)$$

Integrating over the final energy, E_f, gives the differential cross section

$$\frac{d\sigma}{d\Omega} = \int \frac{d^2\sigma}{d\Omega dE_\mathrm{f}} dE_\mathrm{f}. \quad (2.7)$$

The total cross section is found by a double integration:

$$\sigma = \int\int \frac{d^2\sigma}{d\Omega dE_\mathrm{f}} d\Omega dE_\mathrm{f}. \quad (2.8)$$

2.1.4 Beam attenuation due to scattering

Since the number of neutrons scattered is necessarily limited by the number of incoming neutrons, the total cross section cannot be truly proportional to volume, at least not for large, strongly scattering systems. Hence, (2.3) should be understood only as a "thin sample approximation". This equation is valid only when the total scattering cross section of a given sample is much smaller than its area perpendicular to the beam.

In the opposite case, we must consider successive thin slices of thickness dz, each attenuating the incident beam (which we take to travel in the positive z direction):

$$\text{no. of neutrons scattered per sec. from } dz = \Psi(z)\Sigma A(z)dz, \quad (2.9)$$

where $A(z)$ is the area of a sample slice perpendicular to the beam. We assume that the scattering cross section is uniform within the sample and define the attenuation coefficient as

$$\mu = \mu_\mathrm{scatt} = \Sigma, \quad (2.10)$$

The flux of the incident beam in the neutron flight direction is then attenuated inside the sample according to

$$\Psi(z) = \Psi(0)\exp(-\mu z). \tag{2.11}$$

The derivation is simple and is left as an excersize to the reader.

2.1.5 The absorption cross section

Neutron absorption takes place as a result of neutron-induced nuclear processes, which destroys the neutrons, emitting secondary radiation as a result. In most cases, the absorption cross section of thermal neutrons is inversely proportional to the neutron velocity; *i.e.* proportional to the corresponding wavelength, λ.

The neutron absorption cross sections are measured and tabellized for all but the rarest isotopes, see *e.g.* the Neutron Data Booklet, Ref. [13]. Traditionally, the absorption cross sections are given per nucleus in units of "barns" (1 barn $= 10^{-28}$ m^2) and is listed at the typical thermal velocity $v_{\rm th} = 2200$ ms^{-1} (corresponding to $\lambda_{\rm th} = 1.798$ Å). The actual absorption cross section is then given by

$$\sigma_{\rm a} = \sigma_{\rm a,\,th}\frac{v_{\rm th}}{v} = \sigma_{\rm a,\,th}\frac{\lambda}{\lambda_{\rm th}}. \tag{2.12}$$

As in (2.11), the resulting attenuation of the beam is exponential, described by the attenuation coefficient

$$\mu_{\rm a} = \sum_i \frac{N_i\sigma_{{\rm a},i}}{V} = \sum_i n_i\sigma_{{\rm a},i}. \tag{2.13}$$

Here, N is the number of nuclei of the given isotope (labeled i) in the volume V, and $n_i = N_i/V$ is their atomic density. The attenuation coefficients for scattering and absorption are additive, meaning that

$$\mu_{\rm tot} = \mu_{\rm scatt} + \mu_{\rm a}. \tag{2.14}$$

A list of absorption cross sections for selected elements is given in table 2.1.

2.2 Wave description of nuclear scattering

2.2.1 The neutron wave

The incoming (or "initial") neutron can be described as a complex plane wave

$$\psi_{\rm i}(\mathbf{r}) = \frac{1}{\sqrt{Y}}\exp(i\mathbf{k}_{\rm i}\cdot\mathbf{r}), \tag{2.15}$$

where Y is a normalization constant, implying that the density of the incoming neutron is $|\psi_{\rm i}|^2 = 1/Y$. This has no implication on the final results, since Y

Z	Nucleus	b (10^{-15} m)	σ_{inc} (10^{-28} m^2)	$\sigma_{\mathrm{a,th}}$ (10^{-28} m^2)
1	^{1}H	-3.742	80.27	0.3326
1	^{2}D	6.674	2.05	0.000519
2	^{3}He	5.74	1.532	5333
2	^{4}He	3.26	0	0
3	Li	-1.90	0.92	70.5
4	Be	7.79	0.0018	0.0076
5	B	5.30	1.70	767
6	C	6.6484	0.001	0.00350
7	N	9.36	0.50	1.90
8	O	5.805	0	0.00019
9	F	5.654	0.0008	0.0096
10	Ne	4.566	0.008	0.039
11	Na	3.63	1.62	0.530
12	Mg	5.375	0.08	0.063
13	Al	3.449	0.0082	0.231
14	Si	4.1507	0.004	0.171
15	P	5.13	0.005	0.172
16	S	2.847	0.007	0.53
17	Cl	9.5792	5.3	33.5
18	Ar	1.909	0.225	0.675
19	K	3.67	0.27	2.1
20	Ca	4.70	0.05	0.43
21	Sc	12.1	4.5	27.5
22	Ti	-3.37	2.87	6.09
23	V	-0.443	5.08	5.08
24	Cr	3.635	1.83	3.05
25	Mn	-3.750	0.40	13.3
26	Fe	9.45	0.40	2.56
27	Co	2.49	4.8	37.18
28	Ni	10.3	5.2	4.49
29	Cu	7.718	0.55	3.78
30	Zn	5.68	0.077	1.11
32	Ge	8.185	0.18	2.20
48	Cd	4.83	3.46	2520
51	Sb	5.57	0	4.91
58	Cl	4.84	0	0.63
60	Nd	7.69	9.2	50.5
64	Gd	9.5	151	49700
65	Tb	7.34	0.004	23.4
82	Pb	9.401	0.0030	0.171

Table 2.1: Neutron cross sections and scattering length for the first 30 elements (isotopic average using the natural abundancies). In addition, data from heavier elements and selected isotopes are presented. Data taken from [13].

will finally leave the equations, but we keep the normalization for completeness. From (1.4), the particle velocity of a plane neutron wave is

$$v = \frac{\hbar k_{\mathrm{f}}}{m_{\mathrm{n}}}. \tag{2.16}$$

Similarly, the corresponding neutron flux is

$$\Psi_{\mathrm{i}} = |\psi_{\mathrm{i}}|^2 v = \frac{1}{Y}\frac{\hbar k_{\mathrm{i}}}{m_{\mathrm{n}}}. \tag{2.17}$$

2.2.2 Scattering from a single nucleus

The neutrons are scattered by the nucleus by the strong nuclear forces. The range of these forces are femtometers (fm), much smaller than the neutron wavelength (measured in Å). Thus, the neutron cannot probe the internal structure of the nucleus, and the scattering from a single nucleus is, by the first Born approximation, isotropic.

We consider the idealized situation where a neutron with a well defined velocity is scattered by a single nucleus wich is somehow fixed in position. The scattered neutron can be described as a spherical wave leaving the nucleus, which is centered at $\mathbf{r}_j$, as shown in Fig. 2.1. The scattered wave function reads:

$$\psi_{\mathrm{f}}(\mathbf{r}) = \psi_{\mathrm{i}}(\mathbf{r}_j)\frac{-b_j}{|\mathbf{r}-\mathbf{r}_j|}\exp(ik_{\mathrm{f}}|\mathbf{r}-\mathbf{r}_j|), \tag{2.18}$$

where the subscript "f" here means "final". This equation is valid only for $|\mathbf{r}-\mathbf{r}_j| \gg b$, where the *scattering length* b is of the order fm. The minus sign in (2.18) is a convention chosen so that most nuclei will have a positive value of b_j. It should here be noted that strongly absorbing nuclei have an imaginary contributions to the scattering length, which complicates the description. We will, however, not deal with this complication here.

In experiments, r is typically of the order 1 m, while the nuclear coordinate, r_j, is typically of the order 1 mm or less (assumed we place origo close to the centre of the "relevant" part of the sample). Hence, the density of outgoing neutrons can be approximated by $|\psi_{\mathrm{f}}|^2 \approx b_j^2/(Yr^2)$. The number of neutrons per second intersecting a small surface, dA, is $dAv|\psi_{\mathrm{f}}|^2 = dAvb_j^2/(Yr^2)$. Using (2.16) and $d\Omega = dA/r^2$, we reach

$$\text{number of neutrons per second in } d\Omega = \frac{1}{Y}\frac{b^2\hbar k_{\mathrm{f}}}{m_{\mathrm{n}}}d\Omega. \tag{2.19}$$

Since the nucleus is fixed, the scattering must conserve the energy of the neutron, *elastic scattering*, leading to $k_{\mathrm{i}} = k_{\mathrm{f}}$. Using (2.4) and (2.17), this leads to the simple expression for the differential cross section:

$$\frac{d\sigma}{d\Omega} = b_j^2, \tag{2.20}$$

giving the total scattering cross section for a single nucleus

$$\sigma = 4\pi b_j^2. \tag{2.21}$$

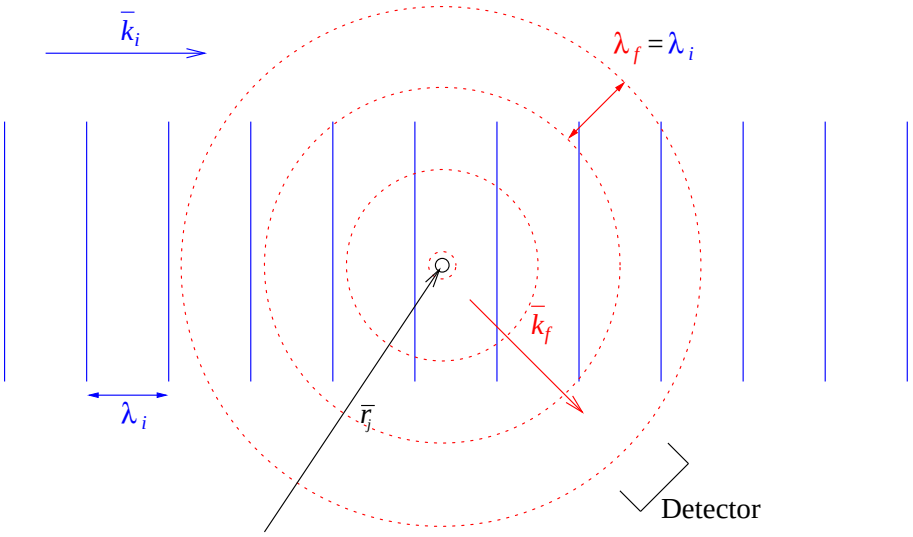

Figure 2.1: An illustration of the initial wave, ψ_{i}, and the final wave, ψ_{f}, describing a neutron scattering off a single nucleus with positive scattering length, b_j. The area, dA, for measuring the flux of the outgoing neutrons is sketched.

Experimental consideration. In the single-neutron normalization we use, the number of scattered neutrons will be much smaller than unity. This should of course be interpreted in the quantum mechanical sense as a probability for this neutron to scatter. Real experiments deals with thousands to billions of neutrons onto the sample per second, so here the probabilities will sum up to give a mean (expected) counting number, N, which can often be considerable. The actual counting number is a stocastical variable, which is approximately follow a normal distribution with mean N and standard deviation $\sqrt{N}$ (meaning that 68% of the times the count value will lie in the interval $N \pm \sqrt{N}$). This approximation is very good for $N > 10$, although it is in practice often used also for smaller couting numbers.

2.2.3 Interference in scattering

In all neutron scattering science, we are concerned with the effect of scattering from a system of scatterers. We now deal with the scattering from two nuclei, labeled j and j', placed at fixed positions. This simple system will reveal some very important features.

The neutron wave that is scattered from the two nuclei is in fact describing just one single neutron. Nevertheless, this neutron "senses" the presence of both nuclei, meaning that the wave scattered from one nucleus will add to the wave scattered from another nucleus. This *interference* is a central aspect in most scattering techniques.

Let us describe this in more precise terms. We assume elastic scattering, $k_\mathrm{i} = k_\mathrm{f} \equiv k$ and identical nuclei, $b_j = b_{j'} \equiv b$. Generalizing (2.18), the outgoing (final) wave can be described as

$$\psi_\mathrm{f}(\mathbf{r}) = -b\left[\frac{\psi_\mathrm{i}(\mathbf{r}_j)}{|\mathbf{r}-\mathbf{r}_j|}\exp(ik|\mathbf{r}-\mathbf{r}_j|) + \frac{\psi_\mathrm{i}(\mathbf{r}_{j'})}{|\mathbf{r}-\mathbf{r}_{j'}|}\exp(ik|\mathbf{r}-\mathbf{r}_{j'}|)\right], \tag{2.22}$$

where $\psi_\mathrm{i}(\mathbf{r})$ is given by (2.15). As before, the two nuclei are assumed to be closely spaced compared with the distance to the observer: $|\mathbf{r}_j - \mathbf{r}_{j'}| \ll r$. Hence, the denominators are equal and we reach

$$\psi_\mathrm{f}(\mathbf{r}) = \frac{1}{\sqrt{Y}}\frac{-b}{r}\left[\exp(i\mathbf{k}_\mathrm{i}\cdot\mathbf{r}_j)\exp(ik|\mathbf{r}-\mathbf{r}_j|) + \exp(i\mathbf{k}_\mathrm{i}\cdot\mathbf{r}_{j'})\exp(ik|\mathbf{r}-\mathbf{r}_{j'}|)\right] \tag{2.23}$$

We now want to calculate the length $|\mathbf{r}-\mathbf{r}_j|$, since it enters the phase of the complex wave function. It is convenient to write the nuclear coordinate, $\mathbf{r}_j$, as a component parallel to and perpendicular to $\mathbf{r}$:

$$|\mathbf{r}-\mathbf{r}_j| = |\mathbf{r}-\mathbf{r}_{j,||}-\mathbf{r}_{j,\perp}| = \sqrt{(\mathbf{r}-\mathbf{r}_{j,||})^2 + (\mathbf{r}_{j,\perp})^2}, \tag{2.24}$$

where the last step is due to Pythagoras. The last term in the square root is small and vanish to first order, meaning that only one nuclear coordinate, $\mathbf{r}_{j,||}$, contributes and that the square root can be lifted to give $|\mathbf{r}-\mathbf{r}_j| = |\mathbf{r}-\mathbf{r}_{j,||}|$. Now, we can write

$$k|\mathbf{r}-\mathbf{r}_{j,||}| = \mathbf{k}_\mathrm{f}\cdot(\mathbf{r}-\mathbf{r}_{j,||}), \tag{2.25}$$

where $\mathbf{k}_\mathrm{f}$ is a wave vector with length $k_\mathrm{f}(=k)$ parallel to $\mathbf{r}$. Finally, we reach

$$\exp(ik|\mathbf{r}-\mathbf{r}_j|) = \exp(i\mathbf{k}_\mathrm{f}\cdot(\mathbf{r}-\mathbf{r}_j)). \tag{2.26}$$

Rearranging terms, the final wave can be written as

$$\psi_\mathrm{f}(\mathbf{r}) = -\frac{1}{\sqrt{Y}}\frac{b}{r}\exp(i\mathbf{k}_\mathrm{f}\cdot\mathbf{r})\left[\exp(i(\mathbf{k}_\mathrm{i}-\mathbf{k}_\mathrm{f})\cdot\mathbf{r}_j) + \exp(i(\mathbf{k}_\mathrm{i}-\mathbf{k}_\mathrm{f})\cdot\mathbf{r}_{j'})\right] \tag{2.27}$$

The intensity of neutrons into a small area is again given as $v|\psi_\mathrm{f}(\mathbf{r})|^2 dA$. This leads to

$$\text{no. of neutrons per sec. in } d\Omega = \frac{1}{Y}\frac{b^2\hbar k_\mathrm{f}}{m_\mathrm{n}}d\Omega\left|\exp(i\mathbf{q}\cdot\mathbf{r}_j) + \exp(i\mathbf{q}\cdot\mathbf{r}_{j'})\right|^2, \tag{2.28}$$

where we have defined the very central concept of neutron scattering, the *scattering vector*, as

$$\mathbf{q} = \mathbf{k}_\mathrm{i} - \mathbf{k}_\mathrm{f}. \tag{2.29}$$

The final expression for the differential scattering cross section now becomes:

$$\frac{d\sigma}{d\Omega} = b^2|\exp(i\mathbf{q}\cdot\mathbf{r}_j) + \exp(i\mathbf{q}\cdot\mathbf{r}_{j'})|^2 = 2b^2\left(1+\cos[\mathbf{q}\cdot(\mathbf{r}_j-\mathbf{r}_{j'})]\right). \tag{2.30}$$

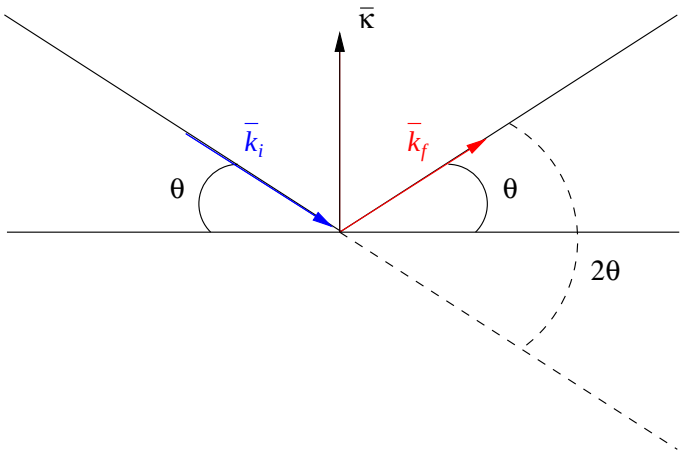

Figure 2.2: An illustration of the scattering process with the incoming and outgoing beam, the wave vectors, $\mathbf{k}_\mathrm{i}$ and $\mathbf{k}_\mathrm{f}$, and the scattering vector q.

At some values of $\mathbf{q}$, this cross section vanish, while at others the value is 4 times that of a single nucleus. This is the essence of interference.

In chapters 5 and 6, we will discuss neutron diffraction from macromolecules and crystals, respectively. These topics essentially deals with interference between waves scattered from a large number of nuclei in the same way as we have seen for two nuclei above.

Experimental considerations In a scattering experiment, one will always measure the *scattering angle* with respect to the incoming beam, as illustrated in Fig. 2.2. The scattering angle is known as 2θ. In elastic scattering, $k_\mathrm{i} = k_\mathrm{f} \equiv k$, and we can see from the figure that

$$q = 2k\sin(\theta). \tag{2.31}$$

2.3 Coherent and incoherent scattering

In a general sample, the neutron scattering length varies from nucleus to nucleus. This can be due to the variation of the nuclear spin direction, or to variation between isotopes of the same element - or between different elements. The latter is a static disorder that for a macrospopic sample can be treated in the same way as a time-dependent disorder, since we can assume the sample is large enough to essentially represent an ensemble average.

In both cases, let us assume that the scattering length at site j has the stocastic value

$$b = \bar{b} + \delta b_j, \tag{2.32}$$

where $\bar{b}$ is shorthand for the average of b and the deviation from the average, δb_j, is assumed independent from site to site. The mean scattering cross section is found from interference terms of the type

$$\left\langle \frac{d\sigma}{d\Omega} \right\rangle = \left\langle |b_j \exp(\mathbf{q}\cdot\mathbf{r}_j) + b_{j'} \exp(\mathbf{q}\cdot\mathbf{r}_{j'})|^2 \right\rangle, \tag{2.33}$$

where the average here means both time and ensemble average. We now see that the "self terms" gives $\langle b_j^2\rangle = \bar{b}_j^2 + \langle \delta b_j^2\rangle$, while the "interference terms" gives $\langle b_j b_{j'}\rangle = \bar{b}_j \bar{b}_{j'}$. We can thus rewrite the equation above

$$\left\langle \frac{d\sigma}{d\Omega} \right\rangle = \frac{\sigma_{\mathrm{inc},j} + \sigma_{\mathrm{inc},j'}}{4\pi} + \left|\bar{b}_j \exp(\mathbf{q}\cdot\mathbf{r}_j) + \bar{b}_{j'} \exp(\mathbf{q}\cdot\mathbf{r}_{j'})\right|^2, \tag{2.34}$$

where $\sigma_{\mathrm{inc}} = 4\pi\langle \delta b_j^2\rangle$ is called the *incoherent scattering cross section*, which represents neutrons emitted in all directions without interference. The average value $\bar{b}$ is denoted the *coherent scattering length*, and $\sigma_{\mathrm{coh}} = 4\pi\bar{b}_j^2$ is the *coherent scattering cross section*.

Usually, the explicit average notation ($\bar{b}$) is dropped, and the symbol b almost exclusively means the average scattering length of a certain isotope or element. This is also the notation used in Table 2.1.

2.3.1 Incoherent nuclear scattering from randomness

One source of incoherent scattering is the spin-dependent term, which is described in detail in [1]. Here, we will deal with incoherent scattering caused by variations in the scattering length due to isotopic mixture or chemical randomness. From the neutron point of view, these two mechanisms are very similar, since they contribute a static random variation in the scattering length profile. The values for the incoherent scattering cross section, found in Table 2.1 deals with the effect from spin and isotopix mixture. For a simple example, assume that the material consists of two isotopes with the abundances $a_c = a$, and $a_d = 1 - a$, and the scattering lengths b_c and b_d, respectively. The average scattering length is

$$\bar{b} = ab_c + (1-a)b_d, \tag{2.35}$$

and the average incoherent cross section can be calculated by an average over the abundances:

$$\begin{aligned} \frac{\sigma_{\mathrm{inc}}}{4\pi} &= \langle (\delta b)^2 \rangle \\ &= a(b_c - \bar{b})^2 + (1-a)(b_d - \bar{b})^2 \\ &= a(1-a)(b_c - b_d)^2. \end{aligned} \tag{2.36}$$

This expression can be generalized to more than two isotopes.

Experimental considerations. The distinction between coherent and incoherent scattering is very important. In most types of experiment you will aim to minimize the incoherent cross section, which creates a uniform background, and maximize the coherent cross section, which generates the features you intent to study. A typical strong source of incoherent scattering is hydrogen, ^{1}H, where the incoherence is due to a strong spin dependence of the interaction between the neutron and the proton.

2.4 Quantum mechanics of scattering

We will now go through the principles of neutron scattering from nuclei in a more strict quantum mechanical way. This section does not contain new results, but may be more satisfactory for readers with a physics background. Further, the formalism developed here carries on to the description of inelastic scattering and magnetic scattering in chapters 7, 8, and 9.

This section is strongly inspired by the treatments in the classical textbooks by Marshall and Lovesey [1] and Squires [2].

2.4.1 The initial and final states

We define the state of the incoming wave as

$$|\psi_\mathrm{i}\rangle = \frac{1}{\sqrt{Y}} \exp(i\mathbf{k}_\mathrm{i} \cdot \mathbf{r}), \tag{2.37}$$

where $Y = L^3$ can now be identified as the normalization volume for the state which is assumed enclosed in a cubic box with a (large) side length L. In stead of the spherical outgoing wave from previous section, we express the final state as (a superposition of) plane waves

$$|\psi_\mathrm{f}\rangle = \frac{1}{\sqrt{Y}} \exp(i\mathbf{k}_\mathrm{f} \cdot \mathbf{r}), \tag{2.38}$$

For these states, we calculate the number density in $\mathbf{k}$-space

$$\frac{dn}{dV_k} = \left(\frac{2\pi}{L}\right)^{-3} = \frac{Y}{(2\pi)^3}. \tag{2.39}$$

We now consider a spherical shell in $\mathbf{k}$-space to calculate the (energy) density of states,

$$\frac{dn}{dE} = \frac{dn}{dV_k}\frac{dV_k}{dk_\mathrm{f}}\left(\frac{dE}{dk_\mathrm{f}}\right)^{-1} = \frac{Y}{(2\pi)^3} 4\pi k_\mathrm{f}^2 \frac{m_\mathrm{n}}{k_\mathrm{f}\hbar^2} = \frac{Y k_\mathrm{f} m_\mathrm{n}}{2\pi^2\hbar^2}, \tag{2.40}$$

an expression we will need in the calculation below.

2.4.2 The master equation for scattering

We describe the interaction responsible for the scattering by the operator $\hat{V}$. The scattering process itself is described by the *Fermi Golden Rule* [15]. This gives the rate of change between the neutron in the single incoming state, $|\psi_\mathrm{i}\rangle$ and a continuum of final states, $|\psi_\mathrm{f}\rangle$.

$$W_{\mathrm{i}\to\mathrm{f}} = \frac{2\pi}{\hbar}\frac{dn}{dE_\mathrm{f}}\left|\left\langle\psi_\mathrm{i}\left|\hat{V}\right|\psi_\mathrm{f}\right\rangle\right|^2, \tag{2.41}$$

where dn/dE_f is the energy density of final states. We wish to consider only neutrons scattered into the solid angle $d\Omega$. Using (2.40), (2.41), and the fraction of the unit sphere, $d\Omega/(4\pi)$, we reach

$$W_{\mathrm{i}\to\mathrm{f},d\Omega} = \frac{Yk_\mathrm{f}m_\mathrm{n}}{(2\pi)^3\hbar^2}d\Omega\left|\left\langle\psi_\mathrm{i}\left|\hat{V}\right|\psi_\mathrm{f}\right\rangle\right|^2. \tag{2.42}$$

We identify $W_{\mathrm{i}\to\mathrm{f},d\Omega}$ with the number of neutrons scattered into $d\Omega$ per second. We now only need an expression for the incoming flux,

$$\Psi = \frac{v}{Y} = \frac{\hbar k_\mathrm{i}}{Ym_\mathrm{n}}, \tag{2.43}$$

to reach the result for the differential scattering cross section (2.4)

$$\begin{aligned}\frac{d\sigma}{d\Omega} &= \frac{1}{\Psi}\frac{W_{\mathrm{i}\to\mathrm{f},d\Omega}}{d\Omega} \\ &= Y^2\frac{k_\mathrm{f}}{k_\mathrm{i}}\left(\frac{m_\mathrm{n}}{2\pi\hbar^2}\right)^2\left|\left\langle\psi_\mathrm{i}\left|\hat{V}\right|\psi_\mathrm{f}\right\rangle\right|^2.\end{aligned} \tag{2.44}$$

In this expression, the normalization volume, Y, will eventually vanish due to the factor $1/\sqrt{Y}$ in the states $|k_\mathrm{i}\rangle$ and $|k_\mathrm{f}\rangle$, since the interactions, $\hat{V}$, are always independent of Y. We will thus from now on neglect the Y dependence in the states and in the cross sections.

Experimental considerations The factor $k_\mathrm{f}/k_\mathrm{i}$ in (2.44) is of importance only for inelastic neutron scattering, where it always appears in the final expressions. For elastic scattering, $k_\mathrm{f} = k_\mathrm{i}$, so the wave vectors divide out.

2.4.3 Elastic nuclear scattering

The interaction between the neutron and the nuclei is expressed by the *Fermi pseudopotential*

$$\hat{V}_j(\mathbf{r}) = \frac{2\pi\hbar^2}{m_\mathrm{n}}b_j\delta(\mathbf{r}-\mathbf{r}_j). \tag{2.45}$$

Here, the spatial delta function represents the short range of the strong nuclear forces and is a sufficient description for the scattering of thermal neutrons.

For a system of a single nucleus, we can now calculate the scattering cross section. We start by calculating the matrix element

$$\begin{aligned}\left\langle \psi_{\mathrm{f}} \left| \hat{V}_j \right| \psi_{\mathrm{i}} \right\rangle &= \frac{2\pi\hbar^2}{m_{\mathrm{n}}} b_j \int \exp(-i\mathbf{k}_{\mathrm{f}} \cdot \mathbf{r}) \delta(\mathbf{r} - \mathbf{r}_j) \exp(i\mathbf{k}_{\mathrm{i}} \cdot \mathbf{r}) d^3\mathbf{r} \quad (2.46) \\ &= \frac{2\pi\hbar^2}{m_{\mathrm{n}}} b_j \exp(i\mathbf{q} \cdot \mathbf{r}_j).\end{aligned}$$

Inserting into (2.44), we reassuringly reach the same results as in (2.20):

$$\frac{d\sigma}{d\Omega} = b_j^2. \quad (2.47)$$

For a system of two nuclei, we can write the scattering potential as a sum $\hat{V} = \hat{V}_j + \hat{V}_{j'}$. In this case, the matrix element becomes

$$\left\langle \psi_{\mathrm{f}} \left| \hat{V} \right| \psi_{\mathrm{i}} \right\rangle = \frac{1}{Y} \frac{2\pi\hbar^2}{m_{\mathrm{n}}} \left(b_j \exp(i\mathbf{q} \cdot \mathbf{r}_j) + b_{j'} \exp(i\mathbf{q} \cdot \mathbf{r}_{j'}) \right). \quad (2.48)$$

Inserting into (2.44), we reach the same result as the simpler approach in section 2.2.

2.4.4 Formalism for inelastic scattering

In some scattering processes, the neutron delivers energy to or absorbs energy from the scattering system. We denote the neutron energy transfer by

$$\hbar\omega = E_{\mathrm{i}} - E_{\mathrm{f}} = \frac{\hbar^2(k_{\mathrm{i}}^2 - k_{\mathrm{f}}^2)}{2m_{\mathrm{n}}}. \quad (2.49)$$

When describing the quantum mechanics of the scattering process, it is important to keep track of the quantum state of the scattering system (the sample), since it may change during the scattering process. The initial and final system states are denoted $|\lambda_{\mathrm{i}}\rangle$ and $|\lambda_{\mathrm{f}}\rangle$, respectively. The partial differential cross section for scattering from $|\lambda_{\mathrm{i}}, \mathbf{k}_{\mathrm{i}}\rangle$ to $|\lambda_{\mathrm{f}}, \mathbf{k}_{\mathrm{f}}\rangle$ is given in analogy with (2.44) by

$$\left.\frac{d^2\sigma}{d\Omega dE_{\mathrm{f}}}\right|_{\lambda_{\mathrm{i}} \to \lambda_{\mathrm{f}}} = \frac{k_{\mathrm{f}}}{k_{\mathrm{i}}} \left(\frac{m_{\mathrm{n}}}{2\pi\hbar^2} \right)^2 \left| \left\langle \lambda_{\mathrm{i}} \psi_{\mathrm{i}} \left| \hat{V} \right| \psi_{\mathrm{f}} \lambda_{\mathrm{f}} \right\rangle \right|^2 \delta(E_{\lambda_{\mathrm{i}}} - E_{\lambda_{\mathrm{f}}} + \hbar\omega), \quad (2.50)$$

where the δ-function expresses explicit energy conservation and the normalization factors Y^2 are omitted.

This expression will be the starting point for us in the chapters on inelastic scattering from lattice vibrations and magnetic excitations.

2.5 Problems

2.5.1 Small questions

1. Derive the exponential decay (2.11).

2. Make your own derivation of the interference between two nuclei (2.30) from (2.23).

3. Why do you think D is often substituted for H in materials, even in cases when the study of the hydrogen itself is not of interest?

2.5.2 Selection of materials for neutron scattering experiments

Most nuclei scatter neutrons incoherently, *i.e.* in random directions. Further, some nuclear isotopes are able to absorb neutrons by nuclear processes. We will now take a closer look at these properties for various materials.

1. Consider the incoherent scattering cross section σ_{inc} for the typical elements occuring in organic materials: H, C, N, O and P. How could one reduce the incoherent background from organic samples?

2. Some transition metals (Sc $\rightarrow$ Zn) display a strong incoherent scattering, and one of them is used as a standard incoherent scatterer (for calibration purposes). Try to figure out which one it is.

3. Sometimes other, more easily accessible, materials are used as incoherent scatterers in stead. Try to suggest one.

4. Which metals may be used for neutron shielding? Calculate the penetration depth $1/\mu$ in these materials for neutron energies of 5 meV. Assume that the number density of atoms in the metal is $1/(16\ \text{Å}^3)$.

5. Also boron nitride, BN, ($V_0 = 11.81\ \text{Å}^3$) is used for shielding purposes. Often, it is used to make adjustable diaphragms (*slits*) to control the size of the neutron beam.

   Calculate the thickness of this material needed to reach an attenuation factor of 10^{-6} for 5 meV neutrons. What will the attenuation then be for 20 meV neutrons?

6. In a neutron scattering experiment, the sample surroundings must be "clean" in the sense of absorption and (incoherent) scattering. Which material would you suggest for constructing cryostats for neutron experiments?

2.5.3 Elastic and inelastic scattering

Describe how the full expression (2.50) for inelastic scattering goes over into the expression (2.44) when the scattering becomes purely elastic.

Chapter 3

Providing neutrons: Sources, moderators, and guides

This experimentally-oriented chapter deals with the production and moderation of research-purpose neutrons. We further discuss how neutrons are transported from the source to the experiments by use of guide systems.

3.1 Neutron sources

A few dozens of neutron sources exist over the World, most of these in Europe and North America. At present, the leading sources are those of ILL (F) and ISIS (UK). Many reactor sources built in the 1960'ies are about to exceed their lifetime and are being closed. Notable recent examples are the reactors at Brookhaven (US), Risø (DK), Studsvik (S), and Jülich (D).

As a new development, advanced reactor and spallation sources are being built and commisioned. I will here mention the new reactors FRM-2 at Technical University of Munich (D), OPAL at ANSTO in Sydney (AUS), and CARR at CIAE (China). Major improvements are being done at ILL, and the second target station at ISIS will double the number of instruments there.

Potentially much more important are the spallation sources SNS, Oak Ridge, Tennessee (first neutrons April 2006; Figure 3.1) and J-PARC in Japan (starting in 2008). An even more ambitious project, the European ESS, is currently under intense discussion with a number of countries offering to host the project, including Spain, Hungary, and Sweden.

In Table 3.1, we list the most important present neutron sources. An updated list of neutron sources Worldwide is found at the home page of the European neutron initiative NMI3.[10]

Figure 3.1: Arial view of the new American "Spallation Neutron Source", SNS. This will become the Worlds most intense pulsed neutron facility.

Name	Location	Type	Power	Commissioning	Instruments
ILL	Grenoble, France	R	58 MW	1971	≈ 50
ORPHEE, LLB	Paris, France	R	14 MW	1982	23
HMI	Berlin, Germany	R	10 MW	1992	20
FRM-2	Munich, Germany	R	20 MW	2004	14
SINQ, PSI	Villigen, Switzerland	CS	800 kW	1996	15
ISIS	Oxfordshire, UK	S	160 kW	1985	$15 \rightarrow 24$
NCNR, NIST	Gaithersburg, MD	R	20 MW	"late 1960'ies"	19
HFIR	Oak Ridge, TN	R	85 MW	1966	14
NRU	Chalk River, Canada	R	125 MW	1957	7
LANSCE	Los Alamos, NM	S	160 kW	19??	13
SNS	Oak Ridge, TN	S	"1.4 MW"	2006	$5 \rightarrow 18$
OPAL, ANSTO	Sydney, Australia	R	20 MW	2007	8
JRR-3M, JAERI	Japan	R	20 MW	?	?
CARR, CIAE	China	R	"60 MW"	20??	?
J-PARC	Japan	S	"1 MW"	2008	?

Table 3.1: Characteristics of significant neutron sources Worldwide, in operation or under construction. Reactor sources are marked by "R" and spallation sources by "S". The continuous spallation source at PSI is denoted "CS".

3.2 Moderators

Neutrons produced by either spallation or reactor sources are very fast, having energies in the MeV regime. To be useful in condensed matter research, the neutrons must be have their energies reduced by many orders of magnitude. This moderation is performed by a large number of successive collisions with a material that scatters strongly, but absorbs weakly. Here, hydrogen (H) is an almost perfect nuclei, also since its low nuclear mass enables it to absorb a large fraction of the neutron energy in each collision.

Most moderators consist of a liquid water (H_2O; 300 K) tank, which will slow neutrons down to roughly thermal equilibrium. When neutrons of lower energies are required, moderators of liquid hydrogen (H_2; 30 K) or solid methane (CH_4; 100 K) are used after the water moderator. At ILL, there is even a hot moderator consisting of graphite at 2000 K. The geometry of the moderator is chosen so that there is no line-of-sight from the primary neutron source to the neutron scattering instruments.

A good introduction to neutron moderator physics is found in Ref. [7].

3.2.1 Energy distribution of moderated neutrons

Neutrons moderated at a temperature, T, will ideally have a distribution of velocities, v, given by the Maxwellian distribution:

$$I(v) \equiv \frac{dN}{dv} = I_0 v^3 \exp\left(-\frac{m_\mathrm{n} v^2}{2k_\mathrm{B}T}\right), \tag{3.1}$$

where N is the total number of neutrons and k_B is Bolzmann's constant. This velocity distribution peaks at $v_\mathrm{max} = \sqrt{3k_\mathrm{B}T/m_\mathrm{n}}$, corresponding to an energy of $3k_\mathrm{B}T/2$.

Is is usual to speak about the "equivalent temperature" of neutrons with a certain energy. The relation is given by

$$E = \frac{m_\mathrm{n} v^2}{2} = k_\mathrm{B} T_\mathrm{equiv}. \tag{3.2}$$

Transfering the Maxwellian distrubution (3.1) in terms of wavelength requires some care. Since $v = 2\pi\hbar/(m_\mathrm{n}\lambda)$, we have $dv = -d\lambda 2\pi\hbar/(m_\mathrm{n}\lambda^2)$. Hence, the wavelength and velocity axes do not scale linearly, and a transformation of the distribution must be applied:

$$I(\lambda) \equiv \frac{dN}{d\lambda} = \frac{dN}{dv}\left|\frac{dv}{d\lambda}\right| = I_0' \lambda^{-5} \exp\left(-\frac{2\pi^2\hbar^2}{\lambda^2 m_\mathrm{n} k_\mathrm{B} T}\right). \tag{3.3}$$

This distribution peaks at $\lambda = 2\pi\hbar\sqrt{3/(5m_\mathrm{n}k_\mathrm{B}T)}$, corresponding to $E = 5k_\mathrm{B}T/3$. The energy equivalent of the peak value is thus changed by some 10% between the two representations of the Maxwellian distribution. Usually, neutron moderator spectra are expressed in terms of the wavelength distribution, as illustrated in Fig. 3.2.

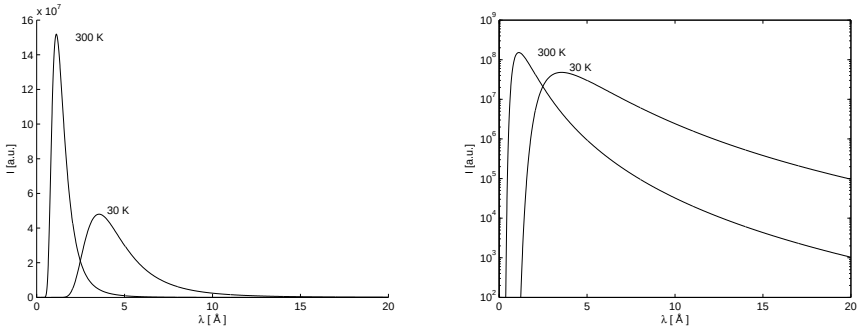

Figure 3.2: Maxwellian wavelength distributions corresponding to typical cold (30 K) and thermal (300 K) sources. Left figure shows a plot with linear axis and right panel shows the intensities on a logarithmic scale.

3.2.2 Realistic description of moderator spectra

To improve transmission, real moderators have a limited thickness and hence do not moderate the neutrons completely. Their velocity distribution should rather be described by two or more Maxwellians, possibly with the addition of a tail towards high energies/low wavelengths, describing neutrons that are scattered only few times in the moderator. This is illustrated for the SINQ source at PSI in Fig. 3.3.

Design and detailed understanding of moderator systems are usually reserved for specialists in this field and is beoynd the scope of these notes. We will here be satisfied with the existence of thermal and cold neutrons sources, and we will from here on deal purely with the utilization of moderated neutrons.

3.3 Neutron guide systems

The earliest neutron scattering instruments used a beam of neutrons, extracted from the moderator through a series of holes in the shielding; also called a beam port. The neutron intensity from this type of beam port falls off in general as $1/r^2$; for details: see problem 3.4.2. This square law dependence dictates that neutron instruments of this type are placed close to the neutron source. Therefore they will suffer from a relatively high background from the source, *e.g.* from fast neutrons.

In the 1970'ies (?), a new concept was invented: The neutron guide. This is a neutron conducting channel that can extract the neutron beam from the moderator and deliver it at another point, further away from the neutron source. Typical guide lengths are 10-100 m.

The neutron guide builds on the principle that surfaces of materials with positive values of b show total reflection of thermal and cold neutrons under sufficiently small angles. At higher angles, the reflectivity falls off to zero very

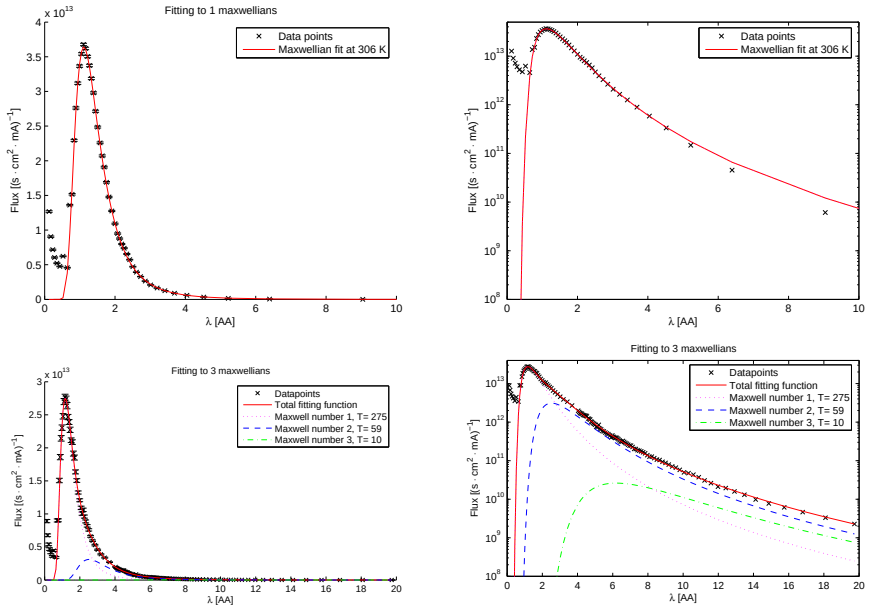

Figure 3.3: Wavelength distributions for SINQ, PSI. Top row shows the measured thermal spectrum (crosses) with a fit to a single Maxwellian at 306 K (solid line). Bottom row shows similar plots for the cold spectrum, with a fit to the sum of three Maxwellians. Both fits have problems for wavelengths below 0.8 Å, where undermoderated (epithermal) neutrons are observed. Left column shows the data on a linear scale, while the right row uses a logarithmic intensity scale.

fast. The physics of this is explained in the chapter on neutron reflectivity (to be written).

We define the *critical* angle, $\theta_c(\lambda)$, as the highest angle between the neutron path and the surface that still gives rise to total reflection. For a given material, the critical angle is proportional to the neutron wavelength. Following Fig. 2.2, the critical scattering vector is now given by

$$Q_c = 2k\sin(\theta_c(\lambda)) \approx 4\pi\frac{\theta_c(\lambda)}{\lambda}. \tag{3.4}$$

In general, Q_c is independent on λ. For the standard guide material, Ni, the critical scattering vector is

$$Q_{c,\mathrm{Ni}} = 0.0219\text{Å}^{-1}. \tag{3.5}$$

For neutrons of 10 Å wavelength, the critical angle from Ni becomes $\theta_c = 1.00°$; an easy relation to remember.

Modern guides are made from multilayer material, usually with Ni as the outmost layer. This ensures total reflectivity up to $Q_{c,\mathrm{Ni}}$. In addition, the

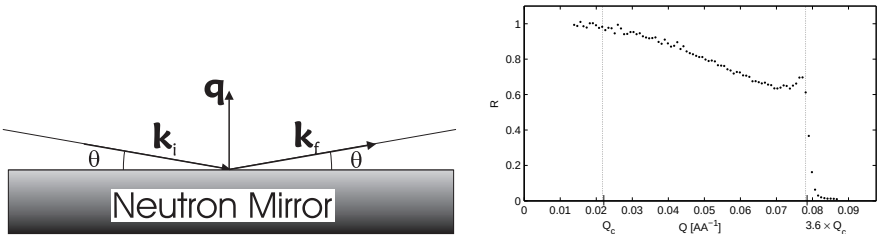

Figure 3.4: Left: The geometry of a neutron reflecting off the surface of a guide. Right: Measured reflectivity profile for a $m = 3$ multilayer guide.

reflectivity is non-zero up to a much higher scattering vector

$$Q_{\mathrm{c}} = mQ_{\mathrm{c,Ni}}. \tag{3.6}$$

One therefore often speaks about the m-value of a multilayer, *e.g.* a $m = 3$ guide, as shown in Fig. 3.4. Typical values of m are 2-4, and multilayer guides can be purchased commercially, typically in pieces of 0.5 m length and cross sections of up to 150×50 mm^2.

Experimental considerations Almost all cold-neutron (and some thermal-neutron) instruments make use of guide systems, which is thus a very general feature of neutron scattering. The remainding part of the instrument, however, may vary significantly, since neutron scattering instruments are highly specialized for different scientific purposes. The general design of typical neutron instruments are presented along with the corresponding scientific topics later in these notes.

In practice, many guides are curved in order to avoid direct line-of-sight from the moderator (or beam port) to the experiment. This is done to further decrease the fast neutron background. At the end of such guides, the background count rates for a typical 150×25 mm^2 detector is typically 0.1 counts/minute with the beam shutter closed; partly due to electronic noise. During an experiment (shutter open), the level of background not originating from the sample is 0.2 counts/minute in the best cases.

For controlling the possibly varying intensities of the beam, *monitors* are used at all neutron instruments for normalization purposes. A monitor is an inefficient detector that interacts with only a small fraction of the neutron beam (of the order 10^{-3} to 10^{-4}). Monitors are typically placed at the end of a guide and (if more beam optical elements are present) just before the sample.

3.4 Problems in basic instrumentation

3.4.1 The moderator

1. In typical neutron scattering experiments, the neutrons are moderated by water. These "thermal" neutrons will (almost) reach thermal equilibrium with the moderator. Calculate the equivalent energy, E, and velocity, v, of a thermal neutron, moderated at $T_{\mathrm{H_2O}} = 300$ K. Calculate the corresponding de Broigle wavelength, λ, and wavenumber, k.

2. Perform the same calculations for neutrons thermalised by liquid H_2 at $T_H = 30$ K.

3. For each of the two types of moderators above, calculate the ratio of intensities at wavelengths of 4 Å and 20 Å.

4. Many neutron instruments utilizes a band of incident wavelength, $\Delta\lambda$. For many instruments, $\Delta\lambda/\lambda$ is almost constant and is of the order 1%-10%, depending on instrument type. For these instruments, calculate the ratio of the neutron flux within this wavelength band at 4 Å and 20 Å.

3.4.2 The beam port

Consider a moderator of a typical useful size of 150×150 mm^2. The moderator emits neutrons isotropically and uniformly over its surface. A beam port of size 50×50 mm^2 is placed 4 m from the moderator face.

Consider a point centered at the moderator-beam port axis; downstream from the beam port. Calculate how the neutron intensity at this point varies with distance, L, from the moderator.

The divergence, η, of a neutron is defined as the angular deviation of the neutron velocity to the "main" axis. Calculate the maximal divergence as a function of L for the case described above.

Hints: The variation in distance between the center and the corners of the moderator or beam port can safely be ignored. Gravity can be neglected.

3.4.3 The neutron guide system

Consider a 20 m Ni ($m = 1$) guide with a constant square cross section 50×50 mm^2, illuminated by a moderator of 150×150 mm^2 at a distance, L.

1. Calculate the critical scattering angle at the guide for 4 Å and 20 Å neutrons.

2. What is the maximal (horizontal or vertical) divergence of neutrons that passes through the guide without being reflected. Compare this to the previous question.

3. A guide is "underilluminated" when the moderator size, not the guide reflectivity, limits the divergence of the tranmitted neutrons in any direction. How close must the guide be at the moderator in order not to be underilluminated at 4 Å and 20 Å wavelengths?

4. The guide entry is placed at $L = 1.5$ m. Compare the neutron flux at $\lambda = 4$ Å at the end of the guide to the flux in the situation where the guide entry is replaced with a beam port of the same size (equivalent to removing the reflecting mirrors from the guide).

5. Can you imagine why guides are not often used for instruments using thermal or hot neutrons?

3.4.4 The collimator

A horizontal collimator consists of a number of thin, parallel, equidistant sheets (like every n'th page in a book) of a neutron absorbing material, so that neutrons traveling in the "wrong" directions are eliminated. The distance between sheets is denoted D and the length of the sheets L.

1. Calculate the transmission, T, as a function of horizontal neutron divergence, η_h (the horizontal deviation from the beam axis). You can assume that the sheets are infinitely thin. Further, assume that the position of individual collimator sheets are unknown (or equivalently that the collimator oscillates sidewards during the experiment).

2. A collimator is described by the FWHM (full width at half maximum) of the transmission curve. Calculate the FWHM in terms of D and L.

3. A typical collimator is 30' (or 0.5°) and has a length of $L = 200$ mm. What is the distance, D, between the absorbing sheets?

4. A 60' collimator is inserted after the guide in 3.4.3 (4). How does that affect the neutron flux for 4 Å and for 20 Å neutrons?

Chapter 4

Monte Carlo simulation of neutron instrumentation

Even in the simplest cases, it is not straightforward to calculate the optics of a neutron guide system. This is illustrated, *e.g.*, by problems 3.4.2 and 3.4.3. An accurate calculation of the properties of a complete and realistic neutron instrument becomes almost hopeless, and various approximations must be performed.

One approach is the approximate, analytical calculations of the instrument resolution function, performed around 1970 by Cooper and Nathans [16] and Popovici [17]. Calculations of this type have been extremely useful for many types of neutron instruments over the past decades, in particular triple-axis spectrometers, which are mostly used for high-precision elastic and inelastic measurements on single crystals.

An alternative way to describe neutron instruments is to perform computer simulations of neutron motion. This can give essentially correct descriptions of neutron instrument models. The results are, however, subject to statistical sampling errors, always present in computer simulations (as in real experiments).

This chapter gives an introduction to Monte Carlo simulations and to existing Monte Carlo ray-tracing packages for neutron scattering. The analytical calculations are (in this version of the notes) not discussed.

4.1 Introduction to the Monte Carlo technique

Monte Carlo simulations is in general a way to approximate multi-dimensional integrals with complex boundary conditions, by use of random sampling. The phrase "Monte Carlo" comes from the generous use of random numbers, which resembles the gambling of the famous Monaco casino. For the history of the Monte Carlo technique, we refer to an excellent essay by one of its inventors [18].

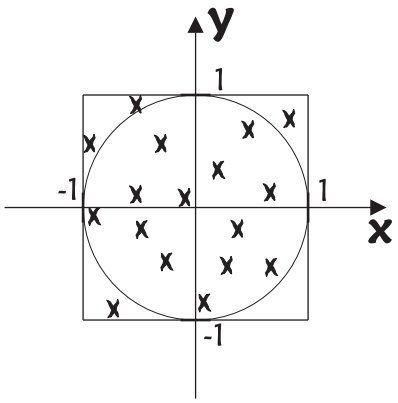

Figure 4.1: A simple example of Monte Carlo simulations. Random points are chosen within the 2×2 square, and the area of the enclosed figure (the unit circle) is estimated from the fraction of points that lie inside the figure. See also the discussion in the text.

As an introduction, consider a simple example. We intent to estimate the area of an object. For simplicity let us consider the unit circle, $x^2 + y^2 \leq 1$, as shown in Fig. 4.1. We now select N points randomly in the square of known area, $A_\mathrm{s} = 4$, that contains the circle fully. The area is defined by

$$-1 \leq x \leq 1 \; ; \; -1 \leq y \leq 1. \tag{4.1}$$

Each of the selected points inside this square is determined by retrieving independent, random values of x and y from a (pseudo-) random number generator. We will not here deal with random number generation, which is described elsewhere [19].

We now calculate the number of points, N_i, that fall inside the unit circle. For large N, the fraction of accepted points will by the law of large numbers approach the ratio of the areas:

$$\frac{N_i}{N} \rightarrow \frac{A_\mathrm{c}}{A_\mathrm{s}}. \tag{4.2}$$

Hence, this "numerical experiment" can be used to estimate the value of the circle area, A_c. Of course, the answer of this example is well known: π.

More complicated calculations may involve complex figures and/or a number of branches (choices between different possibilities). Here, analytical solutions are often impossible, making the Monte Carlo method show its full virtue. One example comes from describing processes in nuclear and particle physics, where the particle under consideration can be either absorbed, scattered, or converted into other particles.

We make no attempt to explain the Monte Carlo technique in detail, but refer to a number of textbooks [12]. In stead, we specialize immediately to the

Package	Origin	Start	Platform	Home page
NISP	Los Alamos (US)	1970'ies	Windows	[20]
IDEAS	Oak Ridge (US)	2000	Windows	[21]
McStas	Risø (DK) and ILL (F)	1999	Unix, Windows, and Mac	[22]
VITESS	HMI (D)	1999	Unix and Windows	[23]
RESTRAX	NPI (CZ)	1996	Unix and Windows	[24]

Table 4.1: Actively developed neutron simulation packages, as of August 2007.

examples relevant for Monte Carlo ray-tracing of neutrons, or similar radiation like electrons or X-rays, which travels along a path (*a ray*) and can either be scattered or absorbed.

4.2 Monte Carlo ray-tracing packages for neutrons

In the early 1990'ies, simulation of the optics in a neutron instrument was performed mostly by monolithic Monte Carlo codes. Although being marvelous pieces of work, these codes were mostly written as one-person projects with limited manpower resources. They were thus subject to lack of generality, possible programming mistakes, low documentation level, and limited user-friendlyness. (One exception from this is the package NISP, see below.)

Now, there exist a number of well-tested and documented general freeware packages for neutron ray-tracing simulations. Each package has the aim of enabling neutron scientists (and students) to quickly set up simulations. The packages development projects co-exist in an atmosphere of collaboration and friendly competition for users. The 5 currently maintained packages are listed in table 4.1; the three European packages are since 2004 supported by the same European research grant [11].

It should be said that the main author of these notes is also a co-author of the McStas package. However, we have kept these notes free from reference to any particular package, to the extent possible.

4.2.1 Describing the neutron optical components

In the simulation packages, the individual optical *components* (or *modules*), like source, guide, sample, and detector, are parametrized and pre-programmed. Each packages contains a library of well-tested components that cover the most often used optical ones, as well as some model samples. It is, however, possible for the user to program additional components upon need. Some of these components may later find their way into the corresponding library, which is thus strengthened by user contributions.

Some of the components contain full quantum mechanical treatment of the neutron as a wave on the microscopic length scales to emulate the correct physics

of the component. However, it should be emphasized that quantum mechanics is only present in the simulations at this level of description. The transport of rays between components is performed by classical kinematics.

4.2.2 Describing the neutron instrument

It is the task of the simulator to assemble the components into a full working instrument. The Monte Carlo simulation itself is then performed by the simulation package on the basis of the instrument description. Most packages have features to visualize the instrument geometry, the simulated rays, and the monitor/detector data, as well as tools for performing multiple simulations, where instrument parameters, *e.g.* rotation angles, are varied.

4.2.3 Virtual experiments

Using a detailed instrument description with a realistic sample model, it is possible to produce a computer model of a complete neutron experiment. This virtual instrument can then be controlled with software that resembles the actual instrument control program, and the simulation data can be analyzed with the same tools as used for real experimental data. This is known as a *virtual experiments*. It is foreseen that virtual experiments can be used to support and complement experimental activities in a number of ways:

- In the design phase of an instrument it can be investigated how the instrument will perform certain key experiment. This can in turn be used to optimize the instrument design.
- When applying for beam time at a facility, the experimentalists can estimate whether the experiment will be feasible at a given instrument and how much beam time is needed.
- Experiments (and experimentalists) can be prepared prior to performing the actual experiment by analyzing the optimal instrument configuration.
- Running experiments can be diagnosed "on the fly" to faster react on various mistakes and errors.
- Analysis of the data can be conducted in more detail by including instrument-related features in the data analysis.
- Students and new users can be trained before their first actual experiment. This is exactly the idea behind the simulation problems in these notes.

4.3 Monte Carlo ray-tracing techniques

All packages have a very similar philosophy in the way simulations are described and performed, and in the way the neutrons are represented. We here describe this in some detail.

4.3.1 Representing the neutrons in simulations

A simulation neutron is represented semiclasically by simultaneously well-defined position, $\mathbf{r}$, velocity, $\mathbf{v}$ and neutron spin vector, $\mathbf{s}$. Formally, this violates the laws of quantum mechanics, in particular the Heisenberg uncertainty relations [15], given for the position/momentum coordinates by

$$\delta x \delta p \geq \frac{\hbar}{2} \tag{4.3}$$

However, as we shall illustrate in problem 4.4.2, the semiclassical approximation is very good for describing instruments that uses "typical" neutrons with velocities of the order 1000 m/s. One important region where the semiclassical approximations breaks down is for very slow (or "ultra-cold") neutrons, where quantum effects becomes prominent in the optical properties.[25]

The neutrons are simulated in "rays", by which we mean the neutron trajectory; position, $\mathbf{r}$, as a function of time, t. Therefore, at any point in the simulation of one ray, t is a necessary parameter. This is of particular importance when simulating pulsed neutron sources.

The validity of the semiclassical approach is discussed in detail in Ref. [26].

4.3.2 The neutron weight factor

To improve simulation speed, a neutron ray in general represents more than a single physical neutron. As a consequence, the ray contains an additional parameter, the *weight factor*, p. This generally has the unit of neutrons per second. When the ray begins at the source, p has a typical initial value of thousands or millions neutrons per second. When some physical neutrons are "lost" due to *e.g.* finite reflectivity or absorption, the simulated rays will in general continue in the simulations, while p is adjusted to reflect the correct average physical behaviour. When a neutron ray reach the detector, p may be only a fraction of a neutron per second.

To quantify this, at a certain point in the simulated instrument, the neutron intensity (again with units neutrons per second) is given by the sum of all rays reaching this point

$$I_j = \sum_{i=1}^{N} p_{i,j} \tag{4.4}$$

where N is the number of simulated rays and j is the index of the given component. If the ray does not reach this point, we take $p_{i,j} = 0$. The weight transformation at a given point in the simulations is expressed by

$$p_j = w_j p_{j-1}, \tag{4.5}$$

where the ray index, i, is omitted for simplicity. The *weight multiplier*, w_j, is calculated by the probability rule

$$f_{\mathrm{MC}} w_j = P, \tag{4.6}$$

where P is the physical probability for the given event, and f_{MC} is the probability that the Monte Carlo simulation selects this event.

Often, there is only one option, $f_{\mathrm{MC}} = 1$, whence $w_j = P$. This is, *e.g.* the case for neutrons being attenuated when passing through absorbing materials. When a Monte Carlo branch point is reached (selection between several events), we have $(f_{\mathrm{MC}})_b < 1$ for each branch, b. However, since f_{MC} is probability function, we must have

$$\sum_b (f_{\mathrm{MC}})_b = 1. \tag{4.7}$$

4.3.3 Scattering from a sample

The place where most Monte Carlo choices are made is when the neutron ray interacts with a sample. It must be decided, whether the ray scatters or not. If scattering takes place, the algorithm must select the point in the sample, the scattered direction, and the final energy. Finally, there is potentially an issue of multiple (repeated) scattering.

To simplify the description, let us just study the scattering direction. Assume we have a sample that only scatters elastically and isotropically with volume specific cross section Σ. Then, the attenuation factor is $\mu = \Sigma$, and the physical probability for scattering is

$$P_{\mathrm{scatt}} = 1 - \exp(-\Sigma L), \tag{4.8}$$

where L is the length of the particular ray within the sample. However, we must also consider the outgoing ray. The probability for scattering into the solid angle $d\Omega$ is

$$P(\Omega)d\Omega = P_{\mathrm{scatt.}} \frac{d\Omega}{4\pi}. \tag{4.9}$$

Assume we require that the ray must always scatter, and select the outgoing ray direction with uniform probability (the "physical way"). Then we have

$$f_{\mathrm{MC\,phys.}} d\Omega = \frac{d\Omega}{4\pi}, \tag{4.10}$$

and (4.6) gives

$$w_{\mathrm{phys.}} = \frac{P(\Omega)d\Omega}{f_{\mathrm{MC\,phys.}} d\Omega} = 1 - \exp(-\Sigma L) \approx \Sigma L, \tag{4.11}$$

where the rightmost approximation is valid only for "thin" samples, $\Sigma L \ll 1$. We have here ignored the attenuation of the outgoing neutron ray.

Some neutron instruments has a geometry such that only rays scattered in certain "interesting directions" have any chance of being detected. In such cases, one will employ the technique of *focusing* to improve simulation efficiency. In focusing, the ray will be emitted only within a certain solid angle, $\Delta\Omega$. (This solid angle must contain all the interesting directions, otherwise the focusing

will give wrong results). Assuming uniform selection within $\Delta\Omega$, the Monte Carlo probability will be given by

$$f_{\mathrm{MC\,focus}} d\Omega = \frac{d\Omega}{\Delta\Omega}, \tag{4.12}$$

and (4.6) gives

$$w_{\mathrm{focus}} = \frac{P_{\mathrm{scatt.}}}{f_{\mathrm{MC\,focus}}} = \frac{\Delta\Omega}{4\pi}(1 - \exp(-\Sigma L)) \approx \frac{\Delta\Omega}{4\pi}\Sigma L, \tag{4.13}$$

comparing to the physical case, the focusing method gives smaller weight factors. This is compensated by a larger number of rays traveling towards the final detector, giving a smaller statistical error on the final result. The mean result will of course be the same using the two methods. In the Monte Carlo simulation literature, the focusing technique will be listed under the headline of *importance sampling*.

4.4 Problems

The simulation part of the present course is based on the package McStas. For technical details about the use of the package, we refer the the user manual found at the home page [22].

The problems below can be solved using the McStas components `Source_simple`, `Source_Maxwell3`, `Slit`, `Guide`, `PSD_monitor`, `Div_monitor`, `L_monitor`, and `Div_L_monitor`. Please note, that in McStas all detectors are denoted monitors.

4.4.1 Estimating the circle area

Construct a simulation with a square neutron source, which emits neutrons in a preferred direction. Focus the source output to a position-sensitive detector, which is much further away than the source size. Verify that the detector is completely illuminated, but that still all emitted neutrons rays are detected. Then place a circular slit very close to the detector.

Use your results to estimate the value of π. Perform the simulations for a varying number of neutron rays, N, in the interval $10^4 - 10^8$. Make a few simulations for each value of N. Estimate how the simulation uncertainty depends on N.

4.4.2 Validity of the semiclassical approximation

Thermal neutrons are considered as classical particles at the instrument level, saving the wave description to the component level. We will now look closer at the the soundness of this semiclassical approximation.

1. In a typical high-angular-resolution experiment to measure diffraction from single crystals, the neutron direction is determined within 10' (10

arc minutes) in the horizontal direction. Consider a set-up, where the neutron energy is 3.7 meV and the beam is limited in space by a slit (or diaphragm) with a width (horizontally) of 1 mm. How does this set-up agree with the uncertainty relations?

2. At the high-energy-resolution neutron scattering instrument SPHERES at FRM-2 (Munich), the neutron energy can be measured with an accuracy of 0.6 μeV, while the neutron energy itself is $E = 1.82$ meV (backscattering from Si analyzer crystals). Similar instruments operate at pulsed neutron sources, where the pulse length is around 10 μs. How does that match the Heisenberg uncertainty relations?

4.4.3 Simulation of incoherent scattering

We will now excercize the rule of weight transformations, (4.6). First, consider a thin sample of an incoherent scatterer, area A, thickness t with $d\Sigma/d\Omega = \rho\sigma_{\rm inc}/(4\pi)$, where ρ is the number density per unit volume and $d\Sigma/d\Omega$ is the differential scattering cross section per unit volume.

1. Show from (2.4) that the scattering probability for a given neutron ray is $P = \sigma_{\rm inc}\rho t$.

2. In a simulation, we choose to focus the neutron rays into an area of $\Delta\Omega$: (a) pick a random direction inside $\Delta\Omega$, (b) scatter all incident neutrons. Argue that the weight factor adjustment should be $w = \rho\sigma_{\rm inc}t\Delta\Omega/(4\pi)$.

3. For a general sample, the cross section per unit volume reads $(d\Sigma/d\Omega)(\mathbf{q})$. argue that the weight factor adjustment will be $w = (d\Sigma/d\Omega)(\mathbf{q})t\Delta\Omega/(4\pi)$, also if the cross section varies with $\mathbf{q}$ across $\Delta\Omega$.

4.5 Simulation project: A neutron guide system

The neutron flux from a moderator can be described by the temperature of a Maxwellian distribution. Assume we have a square cold source 15×15 cm^2 with $T = 30$ K with a neutron flux of 10^{12} neutrons/s/cm^2/steradian. Use this moderator to construct a 20 m neutron guide system with $m = 1$ starting 5 m from the moderator, similar to the one in problem 3.4.3.

1. Simulate this system and try to reproduce the analytical results of problems 3.4.3. Use the McStas guide values $\alpha = 0$, $W = 0$, and $m = 1$ ($m = 0$ to remove the effect of the guide).

2. Exchance the $m = 1$ guide with a multilayer guide of $m = 2$ with the parameters (McStas defaults): $\alpha = 4.38$ and $W = 0.003$. Repeat the simulations to investigate the effect of the new guide material, both with respect to intensity and divergence as a function of neutron wavelength.

Bibliography

[1] W. Marshall and S.W. Lovesey, *Theory of Thermal Neutron Scattering*, Oxford 1971

[2] G.C. Squires, *Thermal Neutron Scattering*, Cambridge University Press, 1978

[3] See the home page of the Nobel Prize committee `www.nobel.se`

[4] D. F. McMorrow and J.-A. Nielsen, *Modern X-ray scattering*, Wiley, 2001

[5] A. Garcia, J.L. Garcia-Luna, G.L. Castro, Phys. Lett. B **500**, 66 (2001)

[6] See also the home pages for the major neutron facilities: `www.ill.fr`, `www.isis.rl.ac.uk`, `www.sns.gov`, `http://j-parc.jp/index-e.html`

[7] G.S. Bauer, *Neutron Sources*, in *Lecture Notes of the Introductory Course to the ECNS99*, Report KFKI-1999-04/E , pp. 12-26

[8] B. Naranjo, J.K. Gimzewski, and S. Putterman, Nature **434**, 1115 (2005)

[9] *** Here should be reference to a paper on neutron detectors ***

[10] See the home page of the NMI3 project `www.neutron-eu.net`

[11] See the home page of the MCNSI part of NMI3 `www.mcnsi.risoe.dk`

[12] D.P. Landau and K. Binder, *A Guide to Monte Carlo Simulations in Statistical Physics*, Cambridge 2005

[13] ILL Neutron Data Booklet, ed. A.-J. Dianoux and G. Lander, 2003

[14] see a review by J.I.l Langford and A.J.C. Wilson, J. Appl. Cryst. **11**, 102 (1978)

[15] E. Merzbacher, *Quantum Mechanics*, Wiley, 1998

[16] M.J. Cooper and R. Nathans, Acta Cryst. **23**, 357 (1967)

[17] M. Popovici, Acta Cryst A **31**, 507 (1975)

[18] N. Metropolis, `http://library.lanl.gov/la-pubs/00326866.pdf`

[19] *** Here should be a paper on random number generation ***

[20] see the NISP home page `www.paseeger.com`

[21] see the IDEAS home page `http://www.ornl.gov/~xwl/publications/NeutronNews-2002.pdf`

[22] see the McStas home page `www.mcstas.org`

[23] see the VITESS home page `www.hmi.de/projects/ess/vitess`

[24] see the RESTRAX home page `omega.ujf.cas.cz/restrax`

[25] V.V. Nesvizhevsky *et al.*, Nature **415**, 297 (2002); R. Golub, Rev. Mod. Phys. **68**, 329 (1996); Y. Hasegawa *et al.*, Nature **425**, 45 (2003)

[26] F. Mezei, *The Basic Physics of Neutron Scattering Experiments*, in *Lecture Notes of the Introductory Course to the ECNS99*, Report KFKI-1999-04/E , pp. 27-39

[27] K. Mortensen, in *Advanced Functional Molecules and Polymers*, ed. H.S. Nalwa, Vol. 2, Overseas Publishers Association, 2001